ICARUS **124,** 698–704 (1996)
ARTICLE NO. 0243

Inertia of Any Polyhedron

ANTHONY R. DOBROVOLSKIS

University of California, Santa Cruz at NASA Ames Research Center, 245-3 Moffett Field, California 94035
E-mail: dobro@cloud9.arc.nasa.gov

Received March 11, 1996; revised August 5, 1996

Simple formulae are given for the surface area, volume, center of mass, moments of inertia, and principal axes of any homogeneous polyhedron. These can easily be combined with algorithms for the gravitational field of such polyhedra. A FORTRAN version of our code (available from the author) is used to compare digital models of Phobos at different resolutions. The results indicate that a surface resolution of about 10° is adequate to characterize the inertial properties of a small satellite or asteroid within a few percent, comparable to the systematic uncertainty for Phobos. This accuracy scales as the square of the resolution. © 1996 Academic Press, Inc.

1. INTRODUCTION

The past decade has seen spacecraft flybys of Uranus and Neptune with their moons of comet Halley, and of asteroids Gaspra and Ida (with its satellite Dactyl). Several asteroids have also been resolved by ground-based radar. As a result, the inventory of Solar System objects with known irregular (nonellipsoidal) shapes has burgeoned from handful of moons to a menagerie of about a dozen-odd assorted small bodies.

The coming decade will be no less active, with flybys of comet Wild 2 and a half-dozen asteroids by the NEAR, Clementine II, Stardust, Rosetta, and New Millenium/Deep Space 1 spacecraft. Furthermore, now that the Arecibo observatory upgrade is nearly complete, we can expect about a dozen asteroid shape determinations by radar each year (or scores if Project Spaceguard is operational; Ostro 1996).

Despite its growing importance, the geophysics of such bodies is in its infancy. Their irregular shapes complicate studies of mass and density, internal structure and composition, photometry and spectrometry, rotation and precession, craters and other surface features, and ejecta and regolith, to name a few. However, considerable progress is being made in several of these areas due in part to recent advances in calculating the gravitational field of an irregular body, modeled as a polyhedron.

A long history distinguishes the central problem of potential theory: to find the gravitational potential of a given body and its gradient, the attraction. Newton showed that the attraction of a spherically symmetric body is the same as if all its mass were concentrated at its center. The gravitational field of a homogeneous ellipsoid has been known in terms of elliptic integrals since 1809 (Ivory). Closed-form expressions for the gravity of a rectangular solid were published in 1930 (MacMillan). There are hints in the literature that the field of an arbitrary polyhedron was studied in the 19th century, but this more general problem did not receive special attention until the last few decades (Bob Werner, personal communication).

The differential potential due to an element of mass d^3M at a distance r from the test point is simply $-Gd^3M/r$, where G is the Newtonian constant of gravitation. The modern approach to the polyhedron depends on the realization that $1/r$ can be represented as the divergence of the vector field $\hat{\mathbf{r}}/2$, where $\hat{\mathbf{r}}$ is the unit vector in the direction from the test point to the mass element (Paul 1974, Barnett 1976, Okabe 1979, Waldvogel 1979, Pohánka 1988, Werner 1994, Werner and Scheeres 1995). Then Gauss' theorem may be applied to transform the integral over all mass elements into an integral over the surface of the body in question. In turn, Green's theorem is used to transform the resulting surface integral over each face of the polyhedron into a line integral around its perimeter. (Apparently Green's theorem in two dimensions is used instead of Stokes' theorem in 3D involving the curl of a vector field, because the divergence of a curl is zero.)

This has applications to geophysics as well as celestial mechanics; for instance, in modeling the gravitational signature of underground masses. A similar method gives the electromagnetic field about a uniformly charged or magnetized polyhedron; this is used, e.g., to interpret the magnetic signal of ore bodies (Barnett 1976, Okabe 1979). Perhaps an analogous approach could also solve the more general problem of the gravitational or electromagnetic interaction between two or more nonspherical bodies.

To complement the solution for the gravitational field, this paper gives simple formulae for the area, volume, centroid, inertia tensor, and principal axes of any homoge-

0019-1035/96 $18.00

neous polyhedron. The inertia tensor is important in the spin dynamics of celestial bodies; for example, the librations of Phobos (Peale 1977), the chaotic rotation of Hyperion (Wisdom *et al.* 1984) and possibly of Nereid (Dobrovolskis 1995), and the precession of Halley's comet (Julian 1990).

Our method uses Gauss' theorem followed by direct integration over the surface to find the inertia tensor. Timmer and Stern (1980) also employed Gauss' theorem, but followed by Green's theorem to compute the surface area, volume, center of mass, and moments of inertia of various objects; their method is exact only when the object is a polyhedron. In contrast, Lien and Kajiya (1984) integrated directly over the volume of a polyhedron to give sophisticated formulae for its inertial properties. In turn, Liggett (1988) applied Green's second identity to express the area, volume, centroid, and moments of inertia for polygons and polyhedra. Finally, Bruner (1995) used Gauss' theorem to find the volume of a polyhedron, but the gradient theorem for its centroid. In general, the previous results are not very accessible.

A FORTRAN version of our code (available from the author) is used to compare digital models of Phobos at different resolutions. The results indicate that a surface resolution of about 10° is adequate to characterize the inertial properties of a small satellite or asteroid within a few percent, comparable to the systematic uncertainty in Phobos' shape. Furthermore, this accuracy varies as the square of the resolution.

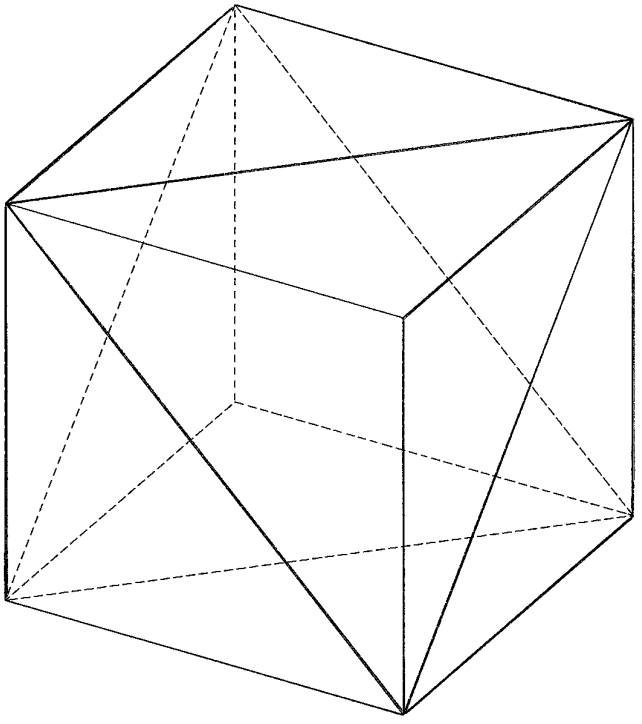

FIG. 1. One possible dissection of the unit cube into a simplicial surface. This particular choice was used to verify the algorithms; we also used the tetrahedron described by the dashed edges.

2. AREA

It is simplest to represent any polyhedron as made up of triangular faces (facets). If the desired surface contains other polygons, we dissect them into triangles before proceeding (see Fig. 1). If the object is described by an array of points, we must first connect the dots into a "simplicial surface" (triangular polyhedron).

Now consider a single facet, whose vertices have position vectors **D**, **E**, and **F**, ordered counterclockwise as seen from outside the body. Next, define the edges (1)

$$\mathbf{G} \equiv \mathbf{E} - \mathbf{D} \quad \text{and} \quad \mathbf{H} \equiv \mathbf{F} - \mathbf{D} \tag{1}$$

(see Fig. 2). By the right-hand rule, their cross product

$$\mathbf{N} \equiv \mathbf{G} \times \mathbf{H} \tag{2}$$

is an outward normal to the facet. Furthermore, the area ΔS of the facet is just half the magnitude of **N**:

$$\Delta S = N/2. \tag{3}$$

Thus the total surface area S of the body is simply the sum of ΔS over all facets. It is noteworthy that the mean silhouette area of a convex body viewed from a random direction (e.g., a tumbling satellite) is one-fourth of its total surface area S.

3. VOLUME

We treat a facet with vertices **D**, **E**, **F** as the base of the solid simplex (tetrahedron) with vertices **D**, **E**, **F**, **0** (see Fig. 2), where the zero vector **0** represents the origin. The volume of a tetrahedron is $\frac{1}{3}$ its height times the area of its base. The altitude of this tetrahedron is the perpendicular distance from the origin to the plane of its base, or the component of **D, E**, or **F** parallel to the surface normal **N**. Thus the volume of the simplex becomes

$$\Delta V = \mathbf{D}/3 \cdot \mathbf{N}/2 = \mathbf{E}/3 \cdot \mathbf{N}/2 = \mathbf{F}/3 \cdot \mathbf{N}/2 \tag{4}$$

or equivalently

$$\Delta V = \mathbf{D}/3 \cdot (\mathbf{G} \times \mathbf{H})/2 = (\mathbf{DEF})/6, \tag{5}$$

where (**DEF**) is the scalar triple product of **D**, **E**, and **F**.

For numerical purposes we evaluate the first of Eqs. (4) above. The total volume V of the body is just the sum of

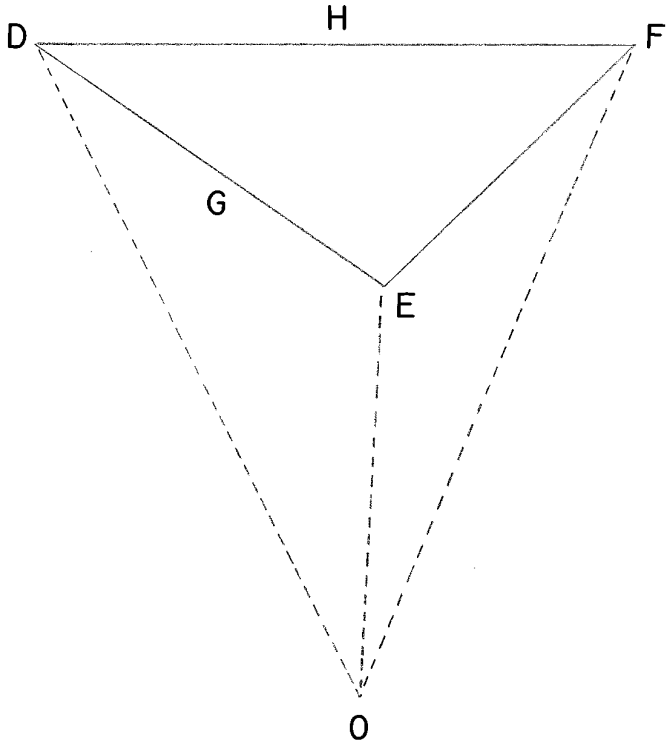

FIG. 2. A facet with vertices **D, E, F** and edges $\mathbf{G} \equiv \mathbf{E} - \mathbf{D}$ and $\mathbf{H} \equiv \mathbf{F} - \mathbf{D}$. The origin is at **0**.

ΔV over all facets. Note that ΔV is negative if the surface normal **N** is directed toward the origin; see Fig. 3.

4. CENTER

Henceforth we assume that the body in question is homogeneous, with uniform density ρ and total mass $M = \rho V$. Then each simplex is also homogeneous, with mass $\Delta M = \rho \Delta \mathrm{V}$. Geometrically, the centroid of any homogeneous triangle lies at the intersection of its median lines (connecting each vertex to the midpoint of the opposite side). Similarly, the centroid of any homogeneous tetrahedron lies at the intersection of its median lines (connecting each vertex to the centroid of the opposite face). In vector terms, the centroid of a simplex [**D**, **E**, **F**, **0**] lies at position

$$\Delta \mathbf{R} = (\mathbf{D} + \mathbf{E} + \mathbf{F} + \mathbf{0})/4 = (\mathbf{D} + \mathbf{E} + \mathbf{F})/4. \qquad (6)$$

This can also be shown by the analytic methods of the following section.

To find the center of mass **R** of the body as a whole, recall that its moment of mass $M\mathbf{R}$ is just the sum of the mass moments $\Delta M\, \Delta \mathbf{R}$ of all the simplices. Thus

$$\begin{aligned} \mathbf{R} &= \sum \Delta M\, \Delta \mathbf{R}/M = \sum \rho \Delta V\, \Delta \mathbf{R}/(\rho V) \\ &= \sum \Delta V\, \Delta \mathbf{R}/V. \end{aligned} \qquad (7)$$

Note that the constant density ρ cancels out of the final expression (7) above. Henceforth ρ can be taken as unity without loss of generality.

5. INERTIA

The rotational inertia of a rigid body may be characterized by its inertia tensor

$$I_{jk} = \begin{bmatrix} I_{xx} & I_{xy} & I_{xz} \\ I_{xy} & I_{yy} & I_{yz} \\ I_{xz} & I_{yz} & I_{zz} \end{bmatrix}. \qquad (8)$$

Note that $I_{jk} = I_{kj}$, so that the inertia tensor is symmetric and involves only six different quantities instead of nine. Furthermore, we express the components of I_{jk} in terms of the products of inertia P_{jk}:

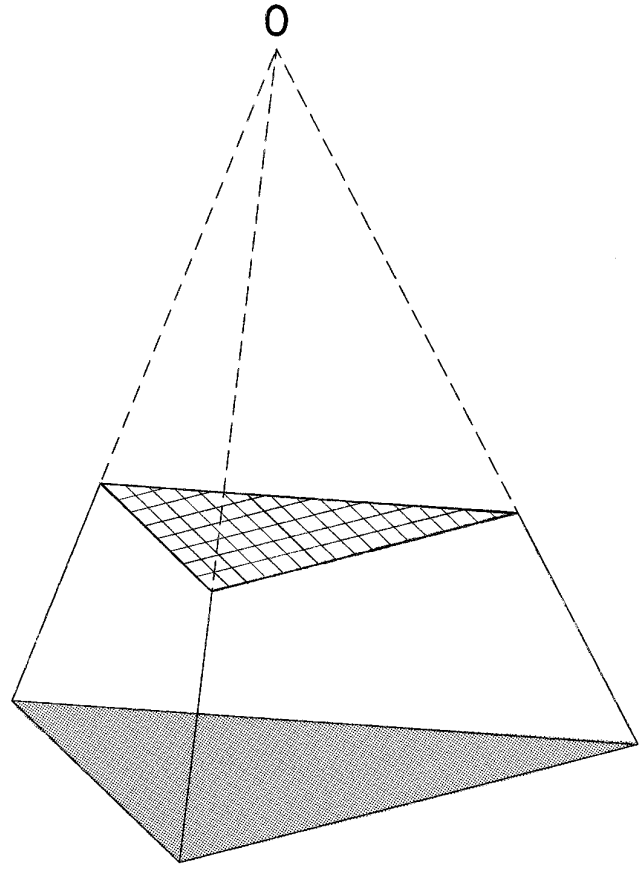

FIG. 3. A truncated pyramid offset from the origin **0**. The cross-hatched triangle faces toward the origin and contributes negative volume ($\Delta V < 0$), while the shaded triangle faces away from the origin and contributes positive volume ($\Delta V > 0$). The three clear faces are radial to the origin and contribute no volume ($\Delta V = 0$).

$$\begin{aligned} I_{xx} &= P_{yy} + P_{zz}, \quad I_{yz} = -P_{yz}, \\ I_{yy} &= P_{xx} + P_{zz}, \quad I_{xz} = -P_{xz}, \\ I_{zz} &= P_{xx} + P_{yy}, \quad I_{xy} = -P_{xy}. \end{aligned} \tag{9}$$

In turn, the products of inertia are defined as

$$\begin{aligned} P_{jk} &\equiv \int\int\int jk\, d^3M = \int\int\int jk\, \rho\, d^3V \\ &= \int\int\int jk\, \rho\, dx\, dy\, dz. \end{aligned} \tag{10}$$

Here the variables j and k each represent a Cartesian coordinate x, y, or z, d^3M is an element of mass, and d^3V is an element of volume.

In general, evaluation of the six integrals P_{jk} above involves some messy algebra, but we can simplify them considerably by use of Gauss' theorem. Given a vector field $\mathbf{Q}$ and its divergence $q = \text{div } \mathbf{Q}$, Gauss' theorem equates the integral of q over a closed volume V to an integral of $\mathbf{Q}$ over its boundary S,

$$\int\int\int q\, d^3V = \int\int \mathbf{Q} \cdot d^2S, \tag{11}$$

where $d^2\mathbf{S}$ is the infinitesimal vector in the direction of the outward normal to S whose magnitude is the element of area $d^2\mathbf{S}$.

To apply (11) above to Eq. (10), we again consider ρ as constant, and take q as jk. For simplicity, we want $\mathbf{Q}$ to be parallel to the radius vector, so that the three radial faces of each simplex do not contribute to the integral. For $q = x^2$, the simplest choice of $\mathbf{Q}$ is $x^2\mathbf{r}/5$; for $q = xy$, the simplest choice of $\mathbf{Q}$ is $xy\,\mathbf{r}/5$. In fact, the simplest choice of $\mathbf{Q}$ turns out to be $jk\mathbf{r}/5$ for all jk. (Compare this with the gravitational problem, where $q = 1/r$ and $\mathbf{Q} = \hat{\mathbf{r}}/2$.)

Now we have for each product of inertia

$$P_{jk} = \frac{\rho}{5}\int\int jk\, \mathbf{r} \cdot d^2\mathbf{S}, \tag{12}$$

where the integral is taken over the nonradial facet. Note that for a simplex,

$$\mathbf{r} \cdot d^2\mathbf{S} = (\mathbf{r} \cdot \mathbf{N}/N)\, d^2S = (6\,\Delta V/N)\, d^2S. \tag{13}$$

Then (12) above becomes

$$\Delta P_{jk} = \rho\frac{6}{5}\frac{\Delta V}{N}\int\int jk\, d^2S. \tag{14}$$

Rather than apply Green's Theorem, as Timmer and Stern (1980) did, we integrate Eq. (14) above directly. Define new dimensionless coordinates (g, h) in the plane of the facet **D**, **E**, **F** such that

$$\mathbf{r} = \mathbf{D} + g\mathbf{G} + h\mathbf{H}. \tag{15}$$

Thus we have $x = D_x + gG_x + hH_x$, $y = D_y + gG_y + hH_y$, $z = D_z + gG_z + hH_z$, and the element of area d^2S becomes $N\, dg\, dh$. Then (14) gives

$$\begin{aligned} \Delta P_{jk} &= \frac{6}{5}\rho\,\Delta V\int\int jk\, dg\, dh \\ &= \frac{6}{5}\rho\,\Delta V\int\int (D_j + gG_j + hH_j) \\ &\quad \times (D_k + gG_k + hH_k) dg\, dh \\ &= \frac{6}{5}\rho\,\Delta V\int\int [D_j D_k + g^2 G_j G_k + h^2 H_j H_k \\ &\quad + g(D_j G_k + D_k G_j) + h(D_j H_k + D_k H_j) \\ &\quad + gh(G_j H_k + G_k H_j)]\, dg\, dh. \end{aligned} \tag{16}$$

Furthermore the limits of integration become $0 < g < 1 - h$, $0 < h < 1$ or $0 < g < 1$, $0 < h < 1 - g$. We find

$$\begin{aligned} \int\int dg\, dh &= \tfrac{1}{2}, \\ \int\int g\, dg\, dh &= \int\int h\, dg\, dh = \tfrac{1}{6}, \\ \int\int g^2 dg\, dh &= \int\int h^2 dg\, dh = \tfrac{1}{12}, \\ \int\int gh\, dg\, dh &= \tfrac{1}{24}. \end{aligned} \tag{17}$$

Substituting the above results into (16) gives

$$\begin{aligned} \Delta P_{jk} = \frac{\rho\,\Delta V}{20}[&12D_jD_k + 2G_jG_k + 2H_jH_k \\ &+ 4(D_jG_k + D_kG_j) + 4(D_jH_k + D_kH_j) \\ &+ G_jH_k + G_kH_j]. \end{aligned} \tag{18}$$

Finally, substituting Eqs. (1) into (18) above and simplifying leaves the more symmetric formula

$$\begin{aligned} \Delta P_{jk} = \frac{\rho\,\Delta V}{20}[&2D_jD_k + 2E_jE_k + 2F_jF_k \\ &+ D_jE_k + D_kE_j + D_jF_k + D_kF_j + E_jF_k + E_kF_j]. \end{aligned} \tag{19}$$

Of course, P_{jk} is just the sum of ΔP_{jk} over all facets.

6. AXES

Now we have the inertia tensor I_{jk} relative to the origin, but in order to find the body's principal moments and axes,

we must find the inertia tensor I'_{jk} relative to the center of mass. For this we use the parallel axis theorem,

$$I'_{jk} = I_{jk} - M \begin{bmatrix} Y^2 + Z^2 & -XY & -XZ \\ -XY & X^2 + Z^2 & -YZ \\ -XZ & -YZ & X^2 + Y^2 \end{bmatrix}, \quad (20)$$

where (X, Y, Z) are the Cartesian components of the center-of-mass vector $\mathbf{R}$.

Note that the inertia tensor I'_{jk} has been translated to a new origin, but still refers to the same coordinate directions. To find its principal axes, we must rotate I'_{jk} into new coordinates where the inertia tensor becomes a diagonal matrix. Then its diagonal elements are the principal moments of inertia, which we label $A \le B \le C$. (Timmer and Stern (1980) did not face this issue, because all of their test objects already had diagonal inertia tensors.) This is a classic eigenvalue problem, with eigenvalues A, B, and C, whose eigenvectors lie along the body's corresponding principal axes. Because I'_{jk} is real and symmetric, its eigenvalues are guaranteed to be real and its eigenvectors to be orthogonal. I'_{jk} is also positive semidefinite, so its eigenvalues must be positive or zero.

In order to solve this eigenproblem, we first find the eigenvalues λ as the roots of the characteristic equation

$$\det L_{jk} = \det I'_{jk} - \lambda \mathrm{II} + \lambda^2 T - \lambda^3 = 0. \quad (21)$$

Here L_{jk} is the singular matrix $(I'_{jk} - \lambda\ \delta_{jk})$, δ_{jk} is the identity matrix, $T = I'_{xx} + I'_{yy} + I'_{zz}$ is the trace of I'_{jk}, and II is its "second invariant":

$$\mathrm{II} = I'_{xx}I'_{yy} + I'_{xx}I'_{zz} + I'_{yy}I'_{zz} - I'^2_{xy} - I'^2_{xz} - I'^2_{yz}. \quad (22)$$

Actually all of the coefficients of the characteristic equation are invariant under coordinate rotations.

Since all of the principal moments are real, the roots of Eq. (21) are

$$\begin{aligned} A &= T/3 - 2U\cos(\theta/3), \\ B &= T/3 - 2U\cos(\theta/3 - 2\pi/3), \\ C &= T/3 - 2U\cos(\theta/3 + 2\pi/3), \end{aligned} \quad (23)$$

where we define

$$U \equiv \sqrt{T^2 - 3\mathrm{II}}/3 \quad (24)$$

and

$$\theta \equiv \mathrm{Arccos}\left(\frac{-2T^3 + 9T\mathrm{II} - 27\det I'_{jk}}{54\,U^3}\right). \quad (25)$$

Now that the eigenvalues are known, the corresponding eigenvectors are easily found. Rather than use a standard eigensystem algorithm, we employ the following strategem. Note that $L_{jk}\mathbf{\Lambda} = \mathbf{0}$, where $\mathbf{\Lambda}$ is the eigenvector corresponding to eigenvalue λ. Then $\mathbf{\Lambda}$ must be orthogonal to each row vector of L_{jk}. Therefore we may find $\mathbf{\Lambda}$ by taking the cross product of two rows of L_{jk}. Note that this trick only works on 3×3 matrices. Furthermore, it will not work if the two row vectors are parallel, or if either one vanishes. To seek a well-defined eigenvector in the numerical algorithm, we form all three cross products of all three pairs of rows.

Each eigenvector represents a principal axis of the body. To each such axis there also corresponds a principal radius, defined as follows. Every inertia tensor is identical to that of an "equivalent ellipsoid" of mass M and principal semiaxes $a \ge b \ge c$, with corresponding moments

$$\begin{aligned} A &= M(b^2 + c^2)/5, \\ B &= M(a^2 + c^2)/5, \\ C &= M(a^2 + b^2)/5. \end{aligned} \quad (26)$$

Solving this system gives the principal radii

$$\begin{aligned} a &= \sqrt{\frac{5(B + C - A)}{2M}}, \\ b &= \sqrt{\frac{5(A + C - B)}{2M}}, \\ c &= \sqrt{\frac{5(A + B - C)}{2M}}. \end{aligned} \quad (27)$$

Note that the volume $\frac{4}{3}\pi abc$ and corresponding density $3M/4\pi abc$ of this ellipsoid only approximate the volume V and density ρ of the original polyhedron. Furthermore, the equivalent ellipsoid is not necessarily the "best-fitting" ellipsoid to the surface. However, the equivalent ellipsoid correctly reproduces the body's rotational inertia, as well as its gravitational quadrupole moments according to MacCullagh's formula (Danby 1962).

In order to verify the coded algorithms, we have reproduced the correct surface area, volume, inertia tensor, and principal axes of several solids, including the cube and tetrahedron in Fig. 1, and a brick (3:2:1). Furthermore, the solutions always satisfy the physical constraint that $C \le A + B$.

7. APPLICATION TO PHOBOS

Here we use our algorithm to show how the inertial properties of a body depend on the resolution of the model. Werner and Scheeres (1995) demonstrated their gravita-

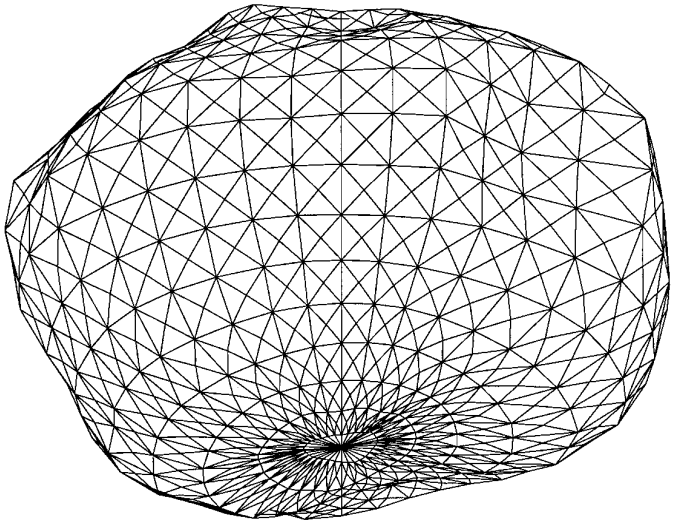

FIG. 4. The 10° model of Phobos, seen from a distant point at 30° south latitude and 90° west longitude. The crater Stickney is visible near the upper right-hand corner.

tional algorithm on a 3300-face digital model of minor planet 4769 Castalia, with a surface resolution of ~5°. However, the poles of Castalia have not both been imaged to this detail. Instead we first applied our algorithm to the same example used by Werner (1994): a simplicial model of Phobos published by Turner (1978), with an equivalent surface resolution of ~15°.

We also used a high-resolution model of Phobos based on more recent data (Simonelli *et al.* 1993), with 16,022 separate points on a 2° × 2° grid of latitude and longitude. We studied degraded versions as well, defined by the subset of points that lie on a 4° × 4° grid, a 10° × 10° grid, and a 20° × 20° grid. In order to apply our algorithm to these models, we first converted each one to a triangular network by inserting a new vertex at the vector mean of every four neighboring points (except at the poles, where the mesh is already triangular, and the surface is oversampled anyway). The resulting 10° × 10° model is displayed in Fig. 4.

The results for all the Phobos models are compared in Table I. For Turner's model, the volume and centroid given by Werner (1994) agree with Table I, while Turner (1978) found a slightly larger volume of 5.62×10^{12} m^3 by an approximate method. For the 2° model, Simonelli *et al.* (1993) found a volume of $(5.74 \pm 0.19) \times 10^{12}$ m^3, in agreement with Table I. In order to find its moments of inertia, Simonelli *et al.* (1993) simply filled their 2° model with a homogeneous distribution of point masses (P. Thomas, personal communication). The resulting principal moments also agree with Table I. Note that the moments of inertia A, B, and C are proportional to the poorly known density ρ.

The eccentricity of its orbit causes Phobos to librate with respect to inertial space by a small angle

$$\delta \approx 5.208^\circ \left[\left(\frac{C}{B - A} \right) - 3 \right]^{-1} \tag{28}$$

(Peale 1977). Our predictions for this quantity are listed in the last row of Table I. Simonelli *et al.* (1993) found

TABLE I
Comparison of Phobos Models

	Model and resolution				
	Simonelli *et al.* (1993)				Turner (1978)
	2°	4°	10°	20°	~15°
Vertices	31,862	7832	1190	272	146
Facets	63,720	15,660	2376	540	288
Edges	95,580	23,490	3564	810	432
S(km^2)	1633	1626	1608	1545	1546
V(km^3)	5750	5737	5666	5377	5404
X(m)	67	65	59	13	−232
Y(m)	−64	−62	−57	−41	63
Z(m)	−52	−51	−49	−18	−191
a(km)	13.048	13.034	12.959	12.640	13.156
b(km)	11.484	11.473	11.417	11.159	10.564
c(km)	9.309	9.305	9.279	9.203	9.337
A/ρ (km^5)	251,301	250,381	245,260	225,017	214,831
B/ρ (km^5)	295,429	294,276	287,834	262,919	281,283
C/ρ (km^5)	347,445	345,956	337,986	305,761	307,690
δ	1.069°	1.067°	1.055°	1.028°	3.195°

$\delta \approx 1.05° \pm 0.19°$ for the 2° model, in agreement with our results. (Turner's 1978 model gives a libration amplitude three times as great, but is based on older data.) The observed amplitude is $\delta \approx 0.8° \pm 0.4°$ (Duxbury and Callahan 1989), consistent with the assumption that Phobos is homogeneous.

Note that the centers of the 2° and 4° models agree within a few meters, while the 10° model differs by ~10 m, and the 20° model departs by almost 70 m. (Turner's 1978 model disagrees with the rest by several hundred meters, but is based on a different data set.) Similarly, the area, volume, principal radii, principal moments, and libration angle all decrease with increasing resolution. This is understandable, because the model was defined using vertices on the surface of Phobos; the actual surface of a rounded body usually bulges outside of such a polyhedral representation.

The trend of all these differences implies that the errors are roughly proportional to the square of the resolution, as can be justified analytically. We have also verified this numerically for polyhedral models of a sphere, an oblate spheroid (2 : 2 : 1), a prolate spheroid (2 : 1 : 1), and a triaxial ellipsoid (4 : 3 : 2). All of these cases indicate that a surface resolution of about 10° should be adequate to characterize the inertial properties of a small satellite or asteroid to a precision within a few percent. This is comparable to the systematic uncertainty in the shape of Phobos (Simonelli *et al.* 1993).

ACKNOWLEDGEMENTS

We thank Peter Thomas for files of the 2° × 2° and 4° × 4° Phobos models, and Daniel Scheeres for a preprint of his paper with Bob Werner. Bob Werner and Damon Simonelli contributed helpful reviews.

REFERENCES

Barnett, C. T. 1976. Theoretical modeling of the magnetic and gravitational fields of an arbitrarily shaped three-dimensional body. *Geophysics* **41,** 1353–1364.

Bruner, C. W. S. 1995. Geometric properties of arbitrary polyhedra in terms of face geometry. *AIAA Journal* **33,** 1350.

Danby, J. M. A. 1962. *Celestial Mechanics.* MacMillan Co., New York.

Dobrovolskis, A. R. 1995. Chaotic rotation of Nereid? *Icarus* **118,** 181–198.

Duxbury, T. C., and J. D. Callahan 1989. Phobos and Deimos control networks. *Icarus* **77,** 275–286.

Ivory, J. 1809. On the attractions of homogeneous ellipsoids. *Philos. Trans. Roy. Soc.* **99,** 345–372.

Julian, W. H. 1990. The Comet Halley nucleus: Random jets. *Icarus* **88,** 355–371.

Lien, S., and J. T. Kajiiya 1984. A symbolic method for calculating the integral properties of arbitrary nonconvex polyhedra. *IEEE Comput. Graphics Appl.* **4,** 35–41.

Liggett, J. A. 1988. Exact formulae for areas, volumes, and moments of polygons and polyhedra. *Comm. Appl. Numer. Methods* **4,** 815–820.

MacMillan, W. D. 1930. *The Theory of the Potential.* McGraw–Hill, New York.

Okabe, M. 1979. Analytical expressions for gravity anomalies due to homogeneous polyhedral bodies and translations into magnetic anomalies. *Geophysics* **44,** 730–741.

Ostro, S. J. 1996. Asteroid radar opportunities with the upgraded Arecibo telescope. In *Abstracts Presented at the International Conference on Asteroids, Comets, and Meteors, Versailles,* p. 64.

Paul, M. K. 1974. The gravity effect of a homogeneous polyhedron for three-dimensional interpretation. *Pure Appl. Geophys.* **112,** 553–561.

Peale, S. J. 1977. Rotation histories of the natural satellites. In *Planetary Satellites,* pp. 87–112. Univ. of Arizona Press, Tucson.

Pohánka, V. 1988. Optimum expression for computation of the gravity field of a homogeneous polyhedral body. *Geophys. Prospecting* **36,** 733–751.

Simonelli, D. P., P. C. Thomas, B. T. Carcich, and J. Veverka 1993. The generation and use of numerical shape models for irregular Solar System objects. *Icarus* **103,** 49–61.

Timmer, H. G., and J. M. Stern 1980. Computation of global geometric properties of solid objects. *Computer-Aided Design* **12,** 301–304.

Turner, R. J. 1978. A model of Phobos. *Icarus* **33,** 116–140.

Waldvogel, J. 1979. The Newtonian potential of homogeneous polyhedra. *Z. Angew. Mathe. Phys.* **30,** 388–398.

Werner, R. A. 1994. The gravitational potential of a homogeneous polyhedron or don't cut corners. *Celest. Mech. Dynam. Astron.* **59,** 253–278.

Werner, R. A., and D. J. Scheeres 1995. Polyhedral gravitation. *Celest. Mech. Dynam. Astron.,* accepted.

Wisdom, J., S. J. Peale, and F. Mignard 1984. The chaotic rotation of Hyperion. *Icarus* **58,** 137–152.